Journal of Colloid and Interface Science
Manuscript Draft

Manuscript Number: JCIS-07-453

Title: Ultrasonic Attenuation Spectroscopy of Emulsions with Droplet Sizes Greater than 10 µm

Article Type: Regular Article

Section/Category: D. Fine Particles, Colloids and Colloidal Stability

Keywords: attenuation spectra; droplet sizes distribution; emulsions; scattering; ultrasonic spectroscopy

Manuscript Region of Origin:

Abstract: Ultrasonic attenuation measurement is a frequently used tool for non-destructive determination of dispersion characteristics. Useful information like particle or droplet size and their concentration can be obtained, if the relation between size and attenuation of the dispersion is known. In this work, the theoretical model by Faran for the intermediate sound wave regime (IWR) is presented in combination with experimental data. In the IWR, the acoustic behavior is governed by elastic scattering rather than by dissipative effects. Experiments with emulsion of droplet sizes greater than 10 µm were carried out. Silicone oil, sunflower oil and olive oil were selected for the disperse phase of the oil-in-water emulsions. First, emulsions having droplets in the micrometer range were created. Afterwards, attenuation measurements of different concentrated emulsion were carried out. Some adjustments reflecting concentration influence were performed to outline the agreement between calculations and measurements. The validity of the model can be confirmed, if the volume fraction of the disperse phase is considered as a variable. Finally, droplet size distributions from theoretical attenuation spectra could be calculated based on a lognormal distribution.

*** 3: Graphical Abstract**

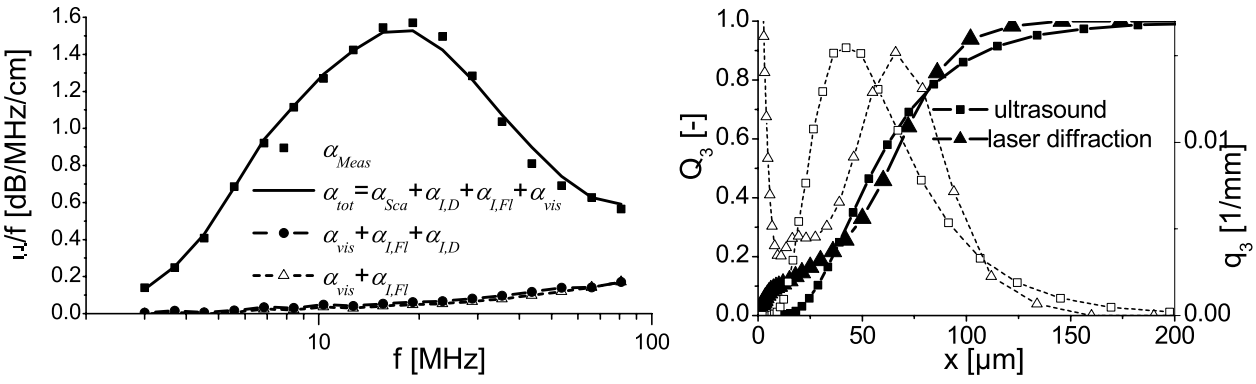

Ultrasonic Attenuation Spectroscopy of Emulsions with Droplet Sizes Greater than 10 µm

Authors:

1. Andreas Richter[*]
2. Tino Voigt[†]
3. Siegfried Ripperger[†]

(Received: March 19th, 2007)

Address for correspondence:

Dipl. Ing. Andreas Richter Institut für Verfahrenstechnik und Umwelttechnik, TU Dresden, 01062 Dresden (Germany), Fon: +49-351-46333500, Fax: +49-351-46337058, Email: ar5@rcs.urz.tu-dresden.de

---

[*]Dipl. Ing. Andreas Richter Institut für Verfahrenstechnik und Umwelttechnik, TU Dresden, 01062 Dresden (Germany),

[†]Dipl.-Ing. Tino Voigt, Prof. Dr.-Ing. Siegfried Ripperger Lehrstuhl für Mechanische Verfahrenstechnik, TU Kaiserslautern, 67663 Kaiserslautern (Germany)

Abstract

Ultrasonic attenuation measurement is a frequently used tool for non-destructive determination of dispersion characteristics. Useful information like particle or droplet size and their concentration can be obtained, if the relation between size and attenuation of the dispersion is known. In this work, the theoretical model by Faran for the intermediate sound wave regime (IWR) is presented in combination with experimental data. In the IWR, the acoustic behavior is governed by elastic scattering rather than by dissipative effects. Experiments with emulsion of droplet sizes greater than 10 µm were carried out. Silicone oil, sunflower oil and olive oil were selected for the disperse phase of the oil-in-water emulsions. First, emulsions having droplets in the micrometer range were created. Afterwards, attenuation measurements of different concentrated emulsion were carried out. Some adjustments reflecting concentration influence were performed to outline the agreement between calculations and measurements. The validity of the model can be confirmed, if the volume fraction of the disperse phase is considered as a variable. Finally, droplet size distributions from theoretical attenuation spectra could be calculated based on a lognormal distribution.

Keywords: attenuation spectra; droplet sizes distribution; emulsions; Scattering; Ultrasonic spectroscopy;

Contents

1 Introduction

In recent years ultrasonic spectroscopy has been established as a fast and reliable method for dispersed system characterization. In particular, the possibility of particle size measurement of highly concentrated or optical opaque dispersions is one of the most important advantages because it allows in-situ process measurements. The first acoustic theory of the behavior of fluid spheres was investigated by Rayleigh [1]. Epstein and Carhart [2] formulated the general principles of sound propagation in dispersed systems by considering mists and fogs. This approach was extended by Allegra and Hawley [3] to include other forms of particulate matter. The combined approach forms the so-called ECAH heory.

Following the development of the ECAH theory many approaches of sound propagation in an ultrasonic field have been developed and described. To distinguish between the applicability of the different theories, the ultrasonic spectrum has been divided into three wavelength regimes. The dimensionless wave number *ka* characterizes the range of the regimes.

$$ka \equiv \frac{2\pi f}{c_{Fl}} a \tag{1.1}$$

Here, a represents the particle or droplet radius, k the wave number and c_{Fl} the fluid sound velocity. Most approaches are only valid in the long wavelength regime ($ka<<1$) [2-4] and restricted to single particle scattering. Attenuation in this region is caused by viscous and thermal loss mechanisms. Besides the ECAH theory, the so-called coupled-phase models have been developed to predict the acoustic behavior of scatterers in the ultrasonic field. These kinds of models are based on the assumption of two abstract phases, one for the combined dispersed matter and one for the

continuous phase. For both phases, balances of continuity, energy and force can be stated and combined into a linear set of equations, under the assumption that time-dependent influences can be neglected. The connection between the formal treatment of two separate phases and the true dispersive state is usually achieved by cell models. The widely used cell model of Dukhin and Goetz [4, [12] considers each particle and the surrounding medium as a single cell, with volume fractions of dispersed and continuous phase chosen according to the dispersion volume distribution. Only thermal and visco-inertial effects along with absorption within the phases are considered in coupled phase models, which limits the applicability of this model type to the long wavelength region.

Since the coupled-phase model and the ECAH theory are available and well understood [2-[4], established frameworks for particle measurement applications in the long wavelength regime have been available. However, if dispersions with larger droplet or particle sizes are considered, ultrasonic attenuation spectroscopy measurements fail due to the lack of universally valid models for the intermediate wavelength regime (IWR).

In this paper the application feasibility of an IWR model for emulsions with droplet sizes larger than 10 µm is demonstrated. The model aspects are outlined, and attenuation calculations are compared to measurements. To obtain measurements, a commercially available ultrasonic attenuation spectrometer was employed.

2 Scattering Theory

Sound attenuation, that is, the decrease of the sound wave amplitude and intensity, occurs in every medium. If obstacles such as a dispersed phase are present in a medium, additional attenuation occurs. A variety of different interaction mechanisms take place between the droplets, the surrounding fluid and the impacting waves. Four basic mechanisms are thought to contribute to attenuation.

- Intrinsic absorption
- Attenuation by thermal coupling of phases
- Attenuation by visco-inertial coupling of phases
- Attenuation by elastic scattering (refraction, diffraction and reflection)

The mechanism of intrinsic absorption can be related to relaxation phenomena within the phases. They are independent of particle or droplet size and are present regardless of wavelength regimes. For describing visco-inertial and thermal attenuation, two significant approaches exist, the ECAH theory [2[3] and the coupled phase/cell models [4[12-[14]. These two types of attenuation modeling frameworks are applicable in the long wavelength regime ($ka \ll 1$).In the intermediate wavelength regime ($ka \sim 1$), however, elastic scattering dominates the propagation of sound. For this regime, both the ECAH theory and the coupled phase models fail because elastic scattering is insufficiently represented.

One theory incorporating elastic scattering was developed by Anderson [8]. For this approach, the derivation is based on a single fixed scatterer, and thus in a way comparable to the ECAH theory. However, effects of viscous coupling of the phases and heat conduction are neglected, which limits the applicability of the approach to the IWR. Furthermore, the Anderson theory fails if solid spheres are considered since only compressional sound waves are allowed.

In solids, shear waves occur in addition to the compressional waves. These waves have been included in the discussion of sound scattering in the model by Faran [10]. The model by Faran is similar to the Anderson model in that it is based on the scattering response of a single particle. Also, by neglecting visco-inertial and thermal effects, the applicability of the theory exhibits the same confinement on the wave regime as the Anderson fluid sphere model. Howevere, an extension of Faran's model to include viscous coupling of the phases exists in the form published by Hay and Mercer [15,[16]. For this approach, visco-inertial effects are considered in the same way as for the ECAH theory. The resulting attenuation coefficients are significantly more complex and require the knowledge of a large number of material properties.

Feuillade and Clay [11] demonstrated numerically that Anderson's theory is a special case of Faran's scattering model, if the shear wave is small. This was demonstrated by calculating the wave velocity and the attenuation coeffient . Therefore, for dispersed systems in which shear waves do not occur, like emulsions, both theories are applicable. Since Faran's theory is the general approach, it is the focal point of the present study.

2.1 Scattering Model

Faran developed the theory of elastic scattering based upon an infinitely long cylinder of isotropic solid material. The same treatment is also applied to spheres, for which the equations and boundary conditions are transformed into spherical coordinates. The geometry for an axially symmetric sound scatter with an incident plane wave is shown in Figure 1.

Figure 1

An incident plane wave approaching along the polar axis can be expressed as

$$p_i(r,\theta) = p_0 \cdot e^{i(k_{Fl} r \cdot \cos\theta - wt)} \\ p_0 \cdot \sum_{n=0}^{\infty} (i)^n \cdot (2n+1) \cdot j_n(k_{Fl} r) \cdot P_n(\cos\theta) \tag{2.1}$$

where p is the sound pressure, $\omega=2\pi f$ the angular frequency and p_0 represents the sound pressure amplitude factor. The wavenumber k_{Fl} of the incident compressional wave is defined by

$$k_{Fl} = \frac{\omega}{c_{Fl}} \tag{2.2}$$

For the outgoing scattered wave just outside the particle, the following relation is assumed:

$$p_{Scat}(r,\theta) = \sum_{n=0}^{\infty} A_n \cdot \left[j_n(k_{Fl} r) + i \cdot n_n(k_{Fl} r) \right] \cdot P_n(\cos\theta) \tag{2.3}$$

with j_n and n_n denoting the spherical Bessel function of the first and second kind, respectively. $P_n(\cos\theta)$ stands for the Legendre polynomial. At large distances from the particle (r>>a) the scattered wave(2.3) takes on the form

$$p_{Scat}(r,\theta) = p_0 \cdot e^{(ik_{Fl} r)} \times \sum_{n=0}^{\infty} (2n+1) \cdot \mathrm{i} \cdot \sin\eta_n \cdot e^{-i\eta} \cdot \frac{P_n(\cos\theta)}{k_{Fl} r} \tag{2.4}$$

The term A_n denotes scattering coefficients which must be obtained through boundary conditions.

Within the elastic scattering approach it is assumed that:

- The pressure in the surrounding fluid is equal to the normal component of stress τ at the body surface.

$$p_{Fl,i,r} + p_{Fl,Scat,r} = \tau_{D,rr} \qquad at\ r = a \tag{2.5}$$

- The normal components of displacement ξ for the fluid and the particle are equal at the body surface.

$$\xi_{Fl,i,r} + \xi_{Fl,Scat,r} = \xi_{D,r} \qquad at\ r = a \tag{2.6}$$

- The tangential component of shear stress must be zero at the surface of the scatterer.

$$[r\theta] = [r\phi] = \tau_{r\theta} = 0 \qquad at\ r = a \tag{2.7}$$

From these boundary conditions, an expression for the scattering coefficient A_n is derived. Following the notation used by Hay and Mercer [16] the scattering coefficient is

$$A_n = \frac{-i \cdot \tan\eta_n}{1 + i \cdot \tan\eta_n} \tag{2.8}$$

The term η_n represents the phase shift of the n-th scattered wave and is defined by the boundary conditions as follows

$$\tan\eta_n = \tan\delta_n(k_{Fl}a) \cdot \frac{\tan\alpha_n(k_{Fl}a) - \frac{\rho_{Fl}}{\rho_D}\tan\zeta_n(k_L a, k_T a)}{\tan\beta_n(k_{Fl}a) - \frac{\rho_{Fl}}{\rho_D}\tan\zeta_n(k_L a, k_T a)} \tag{2.9}$$

with

$$\tan\delta_n(k_{Fl}a) = -\frac{j_n(k_{Fl}a)}{n_n(k_{Fl}a)} \tag{2.10}$$

$$\tan\alpha_n(k_{Fl}a) = -\frac{k_{Fl}a \cdot j_n'(k_{Fl}a)}{j_n(k_{Fl}a)} \tag{2.11}$$

$$\tan\beta_n(k_{Fl}a) = -\frac{k_{Fl}a \cdot n_n'(k_{Fl}a)}{n_n(k_{Fl}a)} \tag{2.12}$$

and

$$\tan\zeta_n(k_La,k_Ta)=\frac{-\frac{(k_Ta)^2}{2}\cdot\left[\frac{\tan\alpha_n(k_La)}{1+\tan\alpha_n(k_La)}-\frac{n^2+n}{n^2+n-1-\frac{(k_Ta)^2}{2}+\tan\alpha_n(k_Ta)}\right]}{\frac{n^2+n-\frac{(k_La)^2}{2}+2\tan\alpha_n(k_La)}{1+\tan\alpha_n(k_La)}-\frac{(n^2+n)\cdot(1+\tan\alpha_n(k_Ta))}{n^2+n-1-\frac{(k_Ta)^2}{2}+\tan\alpha_n(k_Ta)}} \quad (2.13)$$

The dimensionless wave numbers k_La and k_Ta contain the sound velocities $c_{D,L}$ and $c_{D,T}$ of compressional (longitudinal) and shear (transversal) waves in the particle, respectively, while k_{Fl} is a function of the velocity c_{Fl} of the compressional wave in the continuous phase.

Following the derivation of the attenuation coefficient based upon the scattering coefficients, introduced by Hay and Mercer[16, [18] the sound attenuation due to elastic scattering is

$$\alpha=-\frac{3\phi}{2k_{Fl}^2a^3}\sum_{n=0}^{\infty}(2n+1)\,\mathrm{Re}(A_n) \quad (2.14)$$

The dependency of sound attenuation in the intermediate wave regime on dispersed and continuous phase material properties is evident by the presence of the wave velocities of both, the compressional and shear wave velocities and the densities of the phases in the scattering coefficient A_n.

2.2 Droplet Size Distribution Computation from Ultrasonic Attenuation Spectra

Eq. (2.14)] describes the dependency of ultrasound attenuation on frequency f, solids volume fraction ϕ, material properties (through the values in A_n), and a monodispersed droplet size ($a=x/2$). If a size distribution - denoted by the density function $q_3(x)$ - is required to describe the droplet size parameter, the ultrasonic attenuation α_{poly} at frequency f due to the presence of this polydisperse particle ensemble is

$$\alpha_{poly}(f) = \int_{x_{\min}}^{x_{\max}} \alpha(f,x) q_3(x) dx \tag{2.15}$$

due to the superposition of attenuation effects of different size classes [18].If discrete size classes i of with Δx_i and a density distribution $q_3(x_i)$ so that

$$\Delta Q_3(x_i) = q_3(x_i) \cdot \Delta x_i \tag{2.16}$$

and

$$\sum_i \Delta Q_3 = 1 \tag{2.17}$$

are used to specify $q_3(x)$, the integral of Eq. [2.15] can be approximated by a sum [18],

$$\alpha_{poly}(f) \approx \sum_i \alpha(f, x_i) \Delta Q_{3_i} \tag{2.18}$$

Expanding this approach to an attenuation spectrum $\alpha_{poly}(f_j)$ at j frequencies yields

$$\alpha_{poly}(f_j) \approx \sum_i \alpha(f_j, x_i) \Delta Q_{3_i} \tag{2.19}$$

or

$$\boldsymbol{\alpha}_{\mathbf{poly}} \approx \boldsymbol{K} \cdot \boldsymbol{\Delta Q_3}^T \tag{2.20}$$

in matrix notation, with each element of the kernel matrix $\boldsymbol{K}$ defined by $K_{j,i}=\alpha(f_j,x_i)$. This form allows for the calculation of the particle size. Since Eq. (2.20)] is an ill-

posed problem, the inversion of $\boldsymbol{K}$ yields solutions of the size distribution strongly affected by measurement errors. Often, the Phillips-Twomey algorithm is successfully applied [19] to obtain stable solutions with small error.

It is however possible to substitute the inversion step with an estimation of the size distribution based upon a given distribution function type.

Consider again the expression for the attenuation spectrum caused by a discrete size distribution

$$\alpha_{poly}(f_j) \approx \sum_i \alpha\left(f_j, x_i\right) \Delta Q_{3_i} \tag{2.21}$$

Any measured attenuation spectrum $\alpha_{meas}(f_j)$ resulting from the presence of an unknown particle size distribution $\Delta Q_3(x_i)$ can be treated as an estimate for $\alpha_{poly}(f_j)$. An estimate for the size distribution, $\Delta Q_3^*(x_i)$, so that the objective function S attains its minimum,

$$S\left(\Delta Q_3^*\right) = \min_{\Delta Q_3}(\Delta Q_3) \tag{2.22}$$

with

$$S\left(\Delta Q_3\right) = \sum_j e_j{}^2 = \left(\alpha_{meas}(f_j) - \sum_i \alpha\left(f_j, x_i\right) \cdot \Delta Q_3\right)^T \cdot \left(\alpha_{meas}(f_j) - \sum_i \alpha\left(f_j, x_i\right) \cdot \Delta Q_3\right) \tag{2.23}$$

forms the desired particle size distribution vector.

The parameter of the objective function, the size distribution ΔQ_3, can be assumed to follow a defined function type. In the case of a predetermined function, the estimation consists of determining the parameters of the function. For monomodal particle systems, a log-normal size distribution

$$q_3\left(x\right) = \frac{1}{\sigma_{\ln}\sqrt{2\pi}\,x} e^{-\frac{1}{2}\left(\frac{\ln\left(x/x_{50,3}\right)}{\sigma_{\ln}}\right)^2} \tag{2.24}$$

is a valid assumption for the distribution function. For this function type, the minimization problem (Eq. (2.22)]) consists of calculating the median $x_{50,3}$ and standard deviation σ_{ln} . From the values of these parameters, the complete size distribution can be derived.

3 Experimental setup

3.1 Materials

Silicone oil (Wacker AK 50), sunflower oil and olive oil (consumer grade) were employed to form the dispersed phase of the emulsions. The emulsifier used in this study was Tween 80 (polyoxyethylene sorbitan monolaurate). The stabilizer xanthan gum was present in all emulsification experiments. Deionised water was used in the preparation of all solutions. Table 1 lists relevant material properties of all substances.

Table 1

3.2 Emulsifying Apparatus

An injection apparatus was developed for producing emulsions with droplet sizes between 80 and 120 µm. Figure 2 shows the setup of the apparatus.

Figure 2

With an exact volume flow dosage created by an infusion pump the dispersed phase is transported trough the cannula. At the tip, large droplets with diameters of 400 µm are formed due to the inner diameter of the cannula (150µm). The impact of the shear force induced by the stirrer causes additional break-up of droplets, which yields a constant size distribution after an extended stirring period. This resulting droplet size distribution was monitored by laser diffractometry (HELOS, Sympatec GmbH).

Figure 3

Resulting droplet size distributions are shown in Figure 3. Based on the size distributions, it is possible to demonstrate that the mode of the size distribution is in the range from 80 to 100 µm. This size range satisfies the intermediate wave regime (IWR) condition for a frequency range of 1 to 100 MHz (compare Eq [1.1])

3.3 Attenuation Measurement System

For this study, an ultrasonic attenuation spectrometer DT1200 (Dispersion Technology Inc.). The instrument is capable of measuring attenuation over the frequency range from 1 MHz to 100 MHZ by a tone-burst technology employing broadband transducers in an extinction measurement setup.

Figure 4

Figure 4 presents the employed measuring set-up. All experiments were carried out at a temperature of 25 °C. Circulation water was used to regulate the temperature within a margin of ± 0.1 °C. A constant measurement temperature is a prerequisite due to the significant temperature dependence of ultrasonic velocity (2.4 -3 m/(s·°C)) and adiabatic compressibility [20]. To avoid droplet breakup due to pump shear forces, the emulsion circuit was maintained by two stirrers.

4 Methods

4.1 Ultrasonic Attenuation Spectroscopy

Attenuation measurements were carried out for all three oil types. For each emulsion, volume fractions of the dispersed phase were set to φ= 1, 4 and 6 Vol%. The ratio between emulsifier and dispersed volume fraction was set to φ_D/φ_{Em}=1 in every case. At the beginning of each attenuation measurement a calibration run with water was performed to ensure a contamination-free measurement setup. Emulsion measurements were repeated four times to allow for the quantification of the dynamic emulsion behavior. Laser diffraction spectroscopy measurements were carried out in parallel to monitor the size distribution throughout the experiment. Attenuation measurements of the pure liquid phases were performed separately. Averages of at least three measurements were used to define the attenuation spectrum of each substance.

4.2 Data Analysis and Attenuation Predictions

The obtained attenuation spectra were compared with model predictions. Besides the effect of elastic scattering, the measured attenuation spectra of the prepared emulsions also contain a fraction proportional to the absorption of sound within the phase, as well as visco-inertial effects.

For each attenuation mechanism, a model approach needs to be defined to allow for a comparison to measured spectra. The attenuation caused by elastic scattering was modelled based on the elastic scattering theory. Due to the fact that fluid scatterers do not support shear stress propagation, the sound velocity of shear waves $c_{D,T}$ was set to values close to zero (1 m/s). Visco-inertial effects were calculated by the

coupled phase/cell models following the approach of Dukhin and Goetz[4[12]. For the consideration of attenuation by intrinsic absorption, attenuation spectra of the pure phases were integrated into the total calculated attenuation spectrum. These values were obtained from measurements of the pure phase and enter the calculation in direct proportion to the volume fraction of the continuous phase. The total predicted attenuation spectra α_{tot} were created by linear superposition of the contribution by each attenuation mechanism:

$$\alpha_{tot}\left(\varphi_{bf}\right)=\alpha_{Sca}\left(\varphi_{bf}\right)+\alpha_{vis}\left(\varphi_{bf}\right)+\alpha_{I,D}\cdot\varphi_{bf}+\alpha_{I,Fl}\cdot\left(1-\varphi_{bf}\right) \qquad (4.1)$$

Attenuation by scattering is designated by α_{Sca}, whereas attenuation due to visco-inertial losses is described with α_{vis}, and the intrinsic absorption of the dispersed and continuous phase denoted with $\alpha_{I,D}$ and $\alpha_{I,Fl}$.

The determination of droplet size distributions from predicted attenuation spectra comprised of the parameter calculation for a log-normal distribution of the droplet size. The median value $x_{50,3}$, and the standard deviation σ_{ln} were used as fit parameters. The result of this step were size distributions for which the corresponding predicted attenuation showed an optimal agreement with the measured spectra. (see sec. 2.2). The droplet size distributions for each emulsion were then compared with the droplet size distribution determined by laser diffraction spectroscopy.

5 Results and Discussion

5.1 Comparison of Measurements with Predictions

Experimental measurements and theoretical predictions of ultrasonic attenuation at 25 °C are presented in figure 5. The attenuation α/f is plotted against the sound frequency for three different dispersed phase volume fraction and the three different oily phases. Predictions were carried out with the best-fit volume fractions of the dispersed phase φ_{bf}. The attenuation mechanisms contributing to the overall prediction are included in figure 5 to demonstrate their influence (compare Eq. [4.1]). The results indicate that the viscoinertial attenuation α_{vis} amounts to less than 1% of the total attenuation α_{tot}.

Figure 5

The synthetic oil (silicone oil) shows a different attenuation spectrum in comparison with the vegetable oils (sunflower oil, olive oil). A single peak can be observed in the measured spectra of silicone oil, which is absent in other measurements. Furthermore, absolute attenuation values are significantly higher for silicone oil emulsions.

Agreement between model and measurement in the case of silicone oil is good. Here, the prediction suggests that the largest contribution to the overall attenuation is due to elastic scattering. The contribution of other attenuation mechanisms (α_{vis}, $\alpha_{I,D}$, $\alpha_{I,Fl}$) especially in the regions of higher volume fractions is negligible. Table 2 shows that the differences between φ_{nom} and φ_{bf} are small. Deviations from the nominal volume fraction φ_{nom} should be attributed to scale, dosage errors and possible separation effects.

In contrast, the attenuation spectra of the vegetable oil emulsions show a monotonously increasing slope. Total attenuation values are of the same order of magnitude as each of the underlying attenuation mechanisms. Here, attenuation by elastic scattering is not the dominating attenuation effect. Intrinsic losses have more influence on the total attenuation (depending on the dispersed volume fraction). Comparisons between nominal and fitted volume fractions in table 2 show larger deviations than those observed in silicone oil emulsions. These deviations cannot be ascribed to scale, dosage errors or separation effects alone. Instead, a likely reason is the modification of droplet sizes during the experiments. In general, a shift of droplet size distribution leads to an altered scattering behavior and thus to different attenuation coefficients. This effect may have been present in the measurements, possibly caused by the stirring of the emulsions.

To monitor the variation of the droplet size closely, the size distributions were determined during every measurement repetition by laser diffraction spectroscopy. The resulting size distributions varied. On average, the median of the size distribution shifted towards smaller values by 20 µm from the first to the last measurement during a measurement time of 45min. For the calculation of attenuation predictions, only the size distribution recorded at the same time as the ultrasonic attenuation measurements were applied. However, some minor variations of the size distribution which occurred during the 10 minute measurement time frame necessary for ultrasonic attenuation spectroscopy with the DT 1200 instrument are not accounted for.

On the other hand, variation of the dispersed phase volume fraction caused by creaming effects as well as flocculation and consecutive phase separation could lead to a modified measured intrinsic absorption. Additionally, different volume fractions of the dispersed phase could have been present at different locations of the

measurement cell, especially in the region of the ultrasonic transducers. These are moved into the sample cell by an actuator to allow for different measurement gap widths. The result could be a higher droplet concentration beneath or between the transducers due to flow holdup. A comparison of the values in table 2 suggests that the best-fit volume fraction is generally higher than the nominal value.

Furthermore, the simple calculation of the attenuation due to intrinsic absorption as being directly proportional to the volume fraction may be inadequate. An additional simplification was introduced by the separate treatment of intrinsic absorptive and elastic scattering at the droplet. It is very likely that both mechanisms are coupled, because only a part of the sound energy is scattered *into* the droplet while the other part is scattered *away*. At maximum, only the fraction scattered into the droplet can be absorbed, but never the total impacting energy. Absorption in the oil phase thus may be seen as depending on the scattering behavior. In the elastic scattering model approach this could be achieved by incorporating the absorption in the oil phase into the wave number.

$$ka = \frac{2\pi f}{c} a - i \cdot \alpha_{ID} \tag{5.1}$$

For applications other than emulsions, the imaginary part of the wave number is usually negligible because of the small value of α_{ID}.

Furthermore, thermal losses are not considered in the calculation. Temperature gradients appear due to the thermodynamic coupling between pressure and temperature McClements and Povey [14] and Babick et al. [22] showed that thermal losses due to thermodynamic coupling of the phases are of the same order of magnitude as the visco-inertial losses. Therefore, these effects are normally negligible in the regions of larger droplet sizes and higher frequencies discussed

here, but the effect cannot be discounted when discussing the deviations between model and measurements.

At higher dispersed phase volume fractions, particle interactions can occur [5, 18, 23]. In the case of an ensemble of droplets, interactions of scattered waves take place and the single scattering theory is no longer valid for an accurate description of the sound propagation. The widely used multiple scattering theory of Waterman and Truell [24] could be used to consider particle interaction effects within the intermediate wavelength regime.

A final possible reason for discrepancies between measured and predicted attenuation spectra is the fact that natural food oils are not pure substances. Instead, they are mixtures of more than one component. For the calculation of predicted attenuation, mean densities, mean isentropic compressibility and sound speeds are used, which is an approximation of the fluid behavior. The presence of more than one component can lead to different sound propagation and scattering behavior and thus different attenuation spectra.

5.2 Droplet Size Distributions

Cumulative size distributions Q_3 and volume specific density distributions q_3 obtained by laser diffraction and from the best-fit calculation based on the attenuation measurements were plotted against the droplet size.

Figure 6

Figure 6 illustrates that for all silicone oil emulsions good agreement between predicted and measured droplet size distributions can be achieved. However, all density distributions based on the lognormal distribution appear shifted towards smaller droplet sizes.

Small particles agglomerates (< 10μm) of Xanthan gum remaining in the continuous phase could be responsible for the fine fraction of the droplet size distributions. The results from laser diffraction support this explanation in the form of small peaks in density distributions q_3 for small particle sizes. If the log-normal size distribution based on the ultrasonic attenuation spectrum is brought to include this size range as it is the case with the present approximation results, a small shift of the whole distribution function is the result.

Due to its monomodal character, the assumption of a lognormal distribution is not always suitable for the description of a dispersed system. In the case of the vegetable oils unsatisfactory results for the droplet size distributions are obtained. For given measured monotonous attenuation spectra, such as the measurement results for the vegetable oils, more than one size distribution explaining the spectrum exists, leading to ambiguous results.The parameter estimation in this case is not stable and depends on the selected start parameters. An optimization of the estimation process may decrease the ambiguity. Even so, in many cases the sunflower oil emulsion and the olive oil emulsions indicate a size distribution closely reflecting the distribution

measured by laser diffraction. In some cases, the attenuation spectroscopy predictions cover a smaller range of sizes (smaller span of the distribution).However, the median and standard deviation predictions are of the same order of magnitude compared to the laser diffraction results- deviations between size distributions from the different methods should be discussed in light of the method peculiarities.

6 Conclusions

Based upon an experimental study it is shown that attenuation predictions based on a model for elastic scattering matches measurement results for the case of fluid scatterers having sizes of around 100 µm. The relevant model parameters besides size distribution and frequency are sound velocities of the compressional wave in the dispersed and the continuous phase along with the densities of both phases. The model calculations make use of a polydisperse form of the model.

All attenuation measurements were carried out with a commercially available ultrasonic attenuation spectrometer designed for particle sizing applications. Experimental results with silicone oil emulsions show a good agreement with the predictions, supporting the feasibility of the scatteringapproach. Despite a concentration-related deviation for vegetable oil emulsions the agreement between model and measurement is an indication that the scattering approach can be employed to extract particle size information from measured attenuation spectra.

As demonstrated by a best-fit approximation using a log-normal size distribution, the model allows for the size analysis in emulsions with droplet sizes larger than 10 µm.

7 Acknowledgements

The authors would like to express their gratitude to Deutsche Forschungsgemeinschaft (DFG), which supported this work under grant number Nr. RI 776/12.

8 Nomenclature

Symbols:

a	µm	particle radius
A		scattering coefficient
c	m/s	sound velocity
f	MHz	ultrasound requency
k	m^{-1}	wave number
$\boldsymbol{k}$		
j		Bessel function of the first kind
n		Bessel function of the second kind
p	Pa	sound pressure amplitude
P		Legendre polynomial
Q	%	cumulative size distribution
r	m	radial component of vector
S		Objective function
q	m^{-1}	size density distribution
x	m	particle diameter
α	m^{-1}, dB/cm	attenuation coefficent

η		wave phase shift
ϕ		solids volume fraction
θ		angular component of vector
ρ	g/cm^3	density
τ	Pa	stress
σ	m	standard deviation
ω	MHz	angular frequency
ξ	m	displacement

Subscripts

0	initial
3	volume
50	median
bf	best fit
D	droplet
Em	emulsion
Fl	fluid, continuous phase
i	incident
I	intrinsic, absorptive
ln	logarithmic
L	compressional, longitundinal
meas	measured
nom	nominal
poly	polydiserse
r	radial

sca	scattering
tot	total
T	shearing, transversal
vis	viscoinertial
θ	angular component
ϕ	angular component

9 References

[1] Lord Rayleigh, The Theory of Sound. Dover Publications, New York, 1945.

[2] P. S. Epstein, R. R. Carhart, The Absorption of Sound in Suspensions and Emulsions I. Water Fog in Air. J. Acoust. Soc. Am. 25 (1953) 553.

[3] R. Allegra, S. A. Hawley, Attenuation of Sound in Suspensions and Emulsions: Theory and Experiments. J. Acoust. Soc. Am. 51 (1972)1545.

[4] A. S. Dukhin, P. J. Goetz, Acoustic Spectroscopy for Concentrated Polydisperse Colloids with High Density Contrast. Langmuir 12 (1996) 4987.

[5] J. Mobley, K. R. Waters, C. S. Hall, J. N. Marsh, M. S. Hughes, G. H. Brandenburger, J. G. Miller, Measurements and predictions of the phase velocity and attenuation coefficient in suspensions of elastic microspheres. J. Acoust. Soc. Am. 106 (1999) 652.

[6] C. S. Hall, J. N. Marsh, M. S. Hughes, J. Mobley, K. D.Wallace, J. G. Miller, G. H. Brandenburger, Broadband measurements of the attenuation coefficient and backscatter coefficient for suspensions: A potential calibration tool. J. Acoust. Soc. Am. 101 (1997) 1162.

[7] A. E. Hay, A. S. Schaafsma, Resonance scattering in suspensions. J. Acoust. Soc. Am. 85 (1989) 1124.

[8] V. C. Anderson, Sound scattering from a fluid sphere. J. Acoust. Soc. Am. 22 (1950) 426.

[9] R. Hickling and N. M. Wang, Scattering of sound by a rigid movable sphere. J. Acoust. Soc. Am. 39 (1966) 276.

[10] J. J. Faran, Sound Scattering by Solid Cylinders and Spheres. J. Acoust. Soc. Am. 23 (1951) 405.

[11] C. Feuillade and C. S. Clay, Anderson (1950) revisited. J. Acoust. Soc. Am. 106 (1999) 553.

[12] A.S. Dukhin, und P.J. Goetz, Acoustic Spectroscopy for Concentrated Polydisperse Colloids with Low Density Contrast. Langmuir 12 (1996) 4998.

[13] D. J. McClements, Ultrasonic Characterisation of Emulsions and Suspensions. Adv. Colloid Interfaces Sci. 37 (1991) 33.

[14] D. J. McClements and M. J. W. Povey, Scattering of ultrasound by emulsions. J. Phys. D: Appl. Phys. 22 (1989) 38.

[15] A. E. Hay and D. G. Mercer, On the Theory of Sound Scattering and Viscous Absorption in Aqueous Suspension at Medium and Short Wavelengths. J. Acoust. Soc. Am. 78 (1985) 1761.

[16] A.E. Hay and D.G. Mercer, A note on the viscous attenuation of sound in suspensions. J. Acoust. Soc. Am. 85 (1989) 2215.

[17] U. Kräuter, Grundlagen zur in-situ Partikelgrößenanalyse mit Licht und Ultraschall in konzentrierten Partikelsystemen. PhD thesis, University of Karlsruhe, 1995.

[18] A. Richter, F. Babick, S. Ripperger, Polydisperse particle size characterization by ultrasonic attenuation spectroscopy for systems of diverse acoustic contrast in the large particle limit. J. Acoust. Soc. Am. 118 (2005) 1394.

[19] U. Riebel, F. Löffler, The fundamentals of particle size analysis by means of ultrasonic attenuation spectroscopy. Part. Part. Syst. Char. 6 (1989) 135.

[20] D. J. McClements, Ultrasonic Characterizations of Emulsions and Suspensions. Adv. Colloid Interfaces Sci. 37 (1991) 33.

[21] D. J. McClements, Ultrasonic Determination of Depletion Flocculation in Oil-in-Water Emulsions Containing a Non-Ionic Surfactant. Colloids and Surfaces 90 (1994) 25.

[22] F. Babick, F. Hinze, M. Stintz, S. Ripperger, Ultrasonic Spectrometry for Particle Size Analysis in Dense Submicron Suspensions. Part. Part. Syst. Charact. 15 (1998) 230.

[23] U. Riebel, U. Kräuter, Extinction of Radiations in Sterically Interacting Systems of Monodispersed Spheres – Part. 1: Theory. Part. Part. Syst. Charact. 11 (1994) 212.

[24] P. C. Waterman and R. Truell, Multiple Scattering of Waves. J. Math. Phys. 2 (1961) 512.

10 Legends of Illustration

Fig 1: Geometry and coordinate definition of a spherical scatterer in an inviscid fluid

Fig 2: Emulsifying apparatus

Fig 3: Droplet size distribution of emulsion samples containing silicon oil, sunflower oil or olive oil as dispersed phase at a volume concentration of φ=4 Vol% .

Fig 4: Ultrasonic measurement setup used for attenuation experiments.

Fig 5: Comparison between experimental and theoretical values of attenuation spectra α/f against f for a series of three different volume fraction and three different oil-in-water emulsions

Fig 6: Cumulative size distributions Q_3 and density distributions q_3 of investigated emulsions measured by laser diffraction and calculated from ultrasonic attenuation measurements.

5: Figure 1

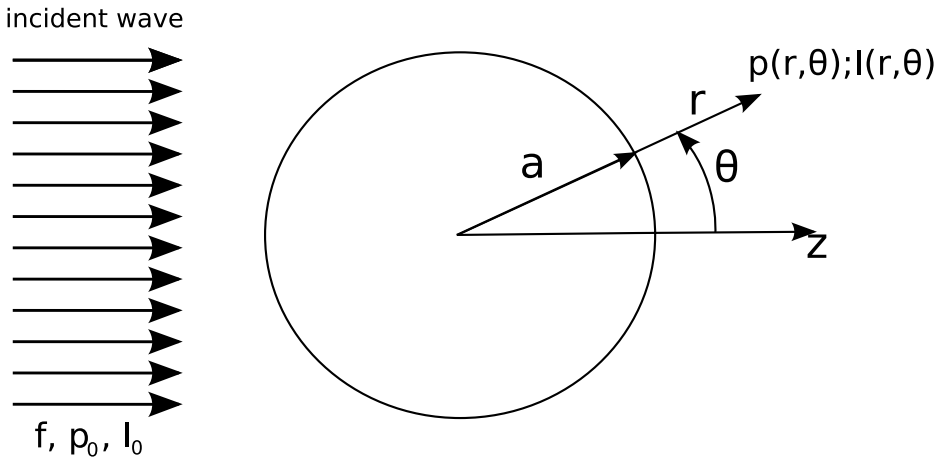

5: Figure 2

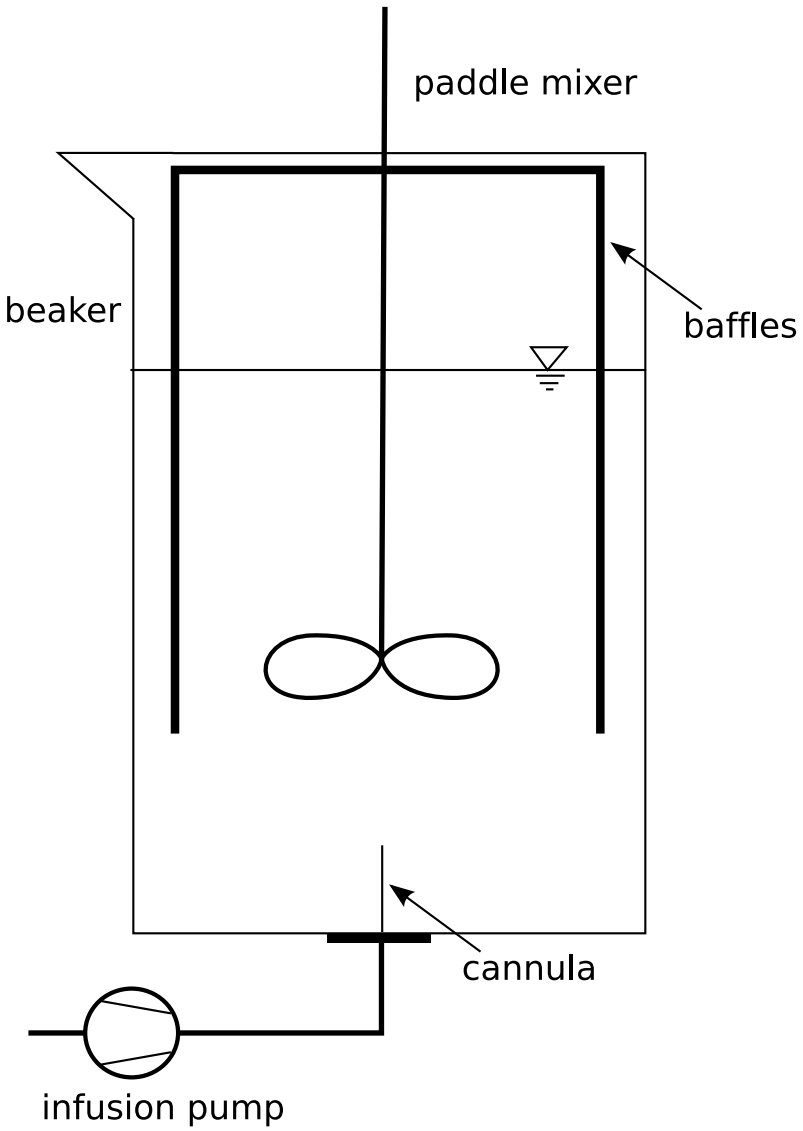

5: Figure 3

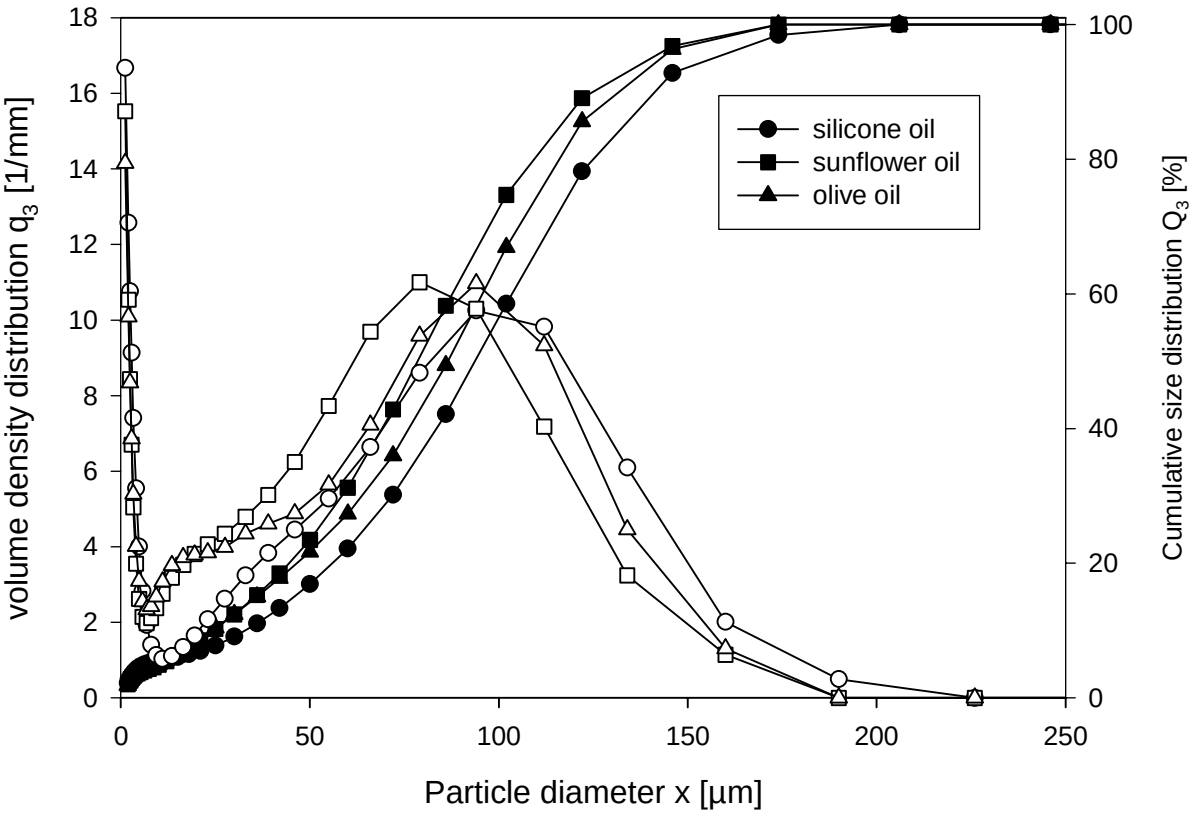
volume density distribution q_3 [1/mm]
Cumulative size distribution Q_3 [%]
Particle diameter x [µm]
silicone oil
sunflower oil
olive oil
0
2
4
6
8
10
12
14
16
18
0
20
40
60
80
100
0
50
100
150
200
250

5: Figure 4

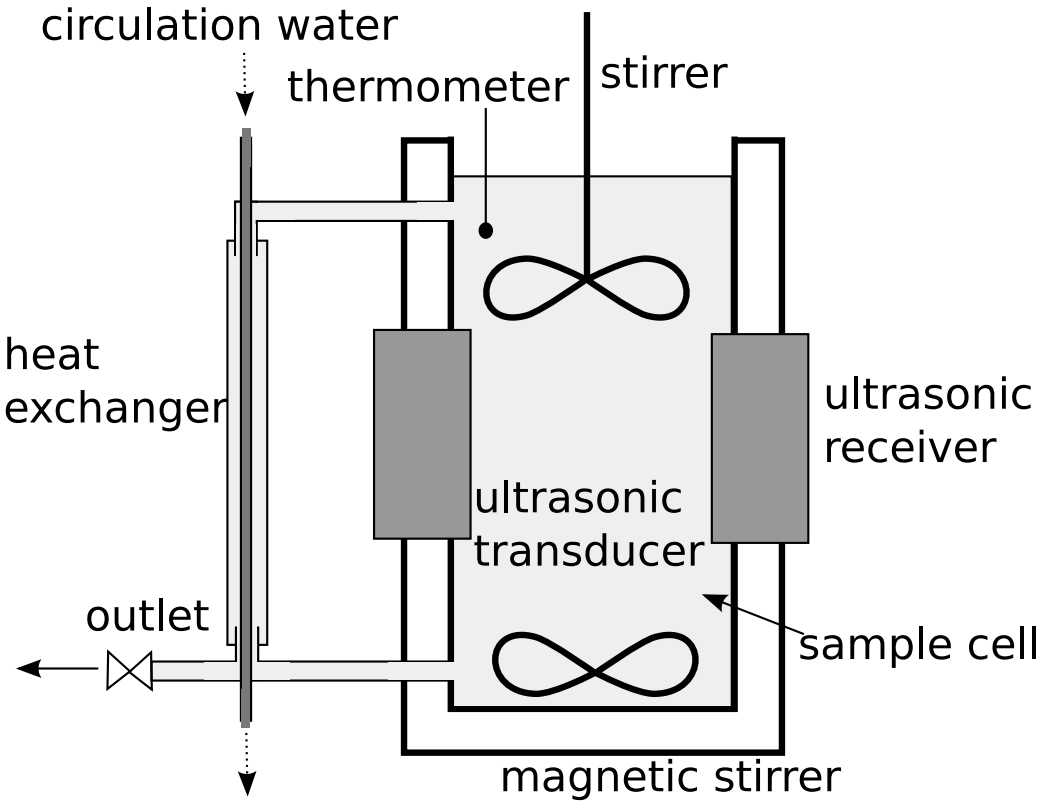
circulation water
thermometer
stirrer
heat
exchanger
ultrasonic
receiver
ultrasonic
transducer
outlet
sample cell
magnetic stirrer

5: Figure 5

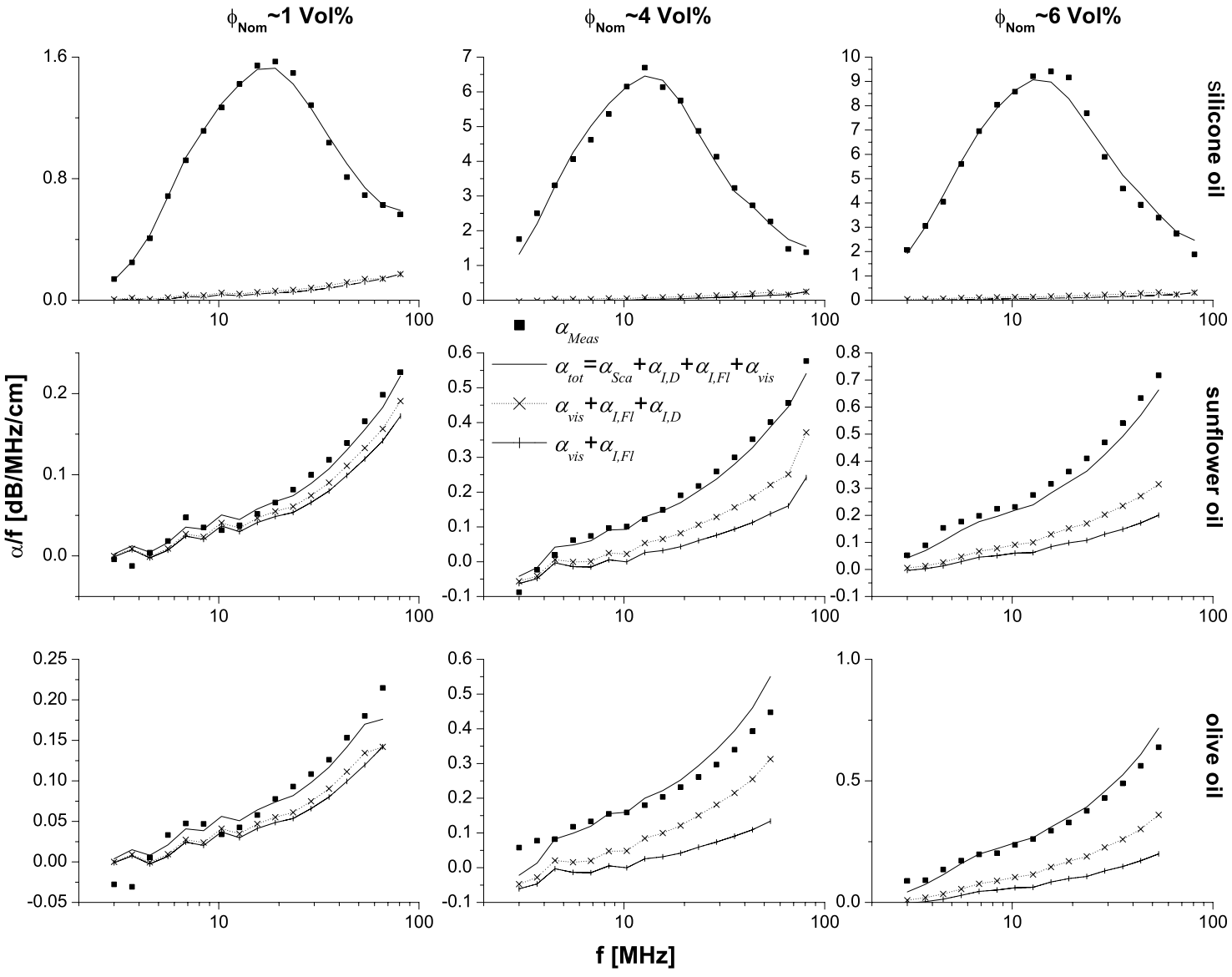
ϕNom~1 Vol%
ϕNom~4 Vol%
ϕNom~6 Vol%
silicone oil
sunflower oil
olive oil
α/f [dB/MHz/cm]
f [MHz]
α_Meas
α_tot=α_Sca+α_I,D+α_I,Fl+α_vis
α_vis+α_I,Fl+α_I,D
α_vis+α_I,Fl

5: Figure 6

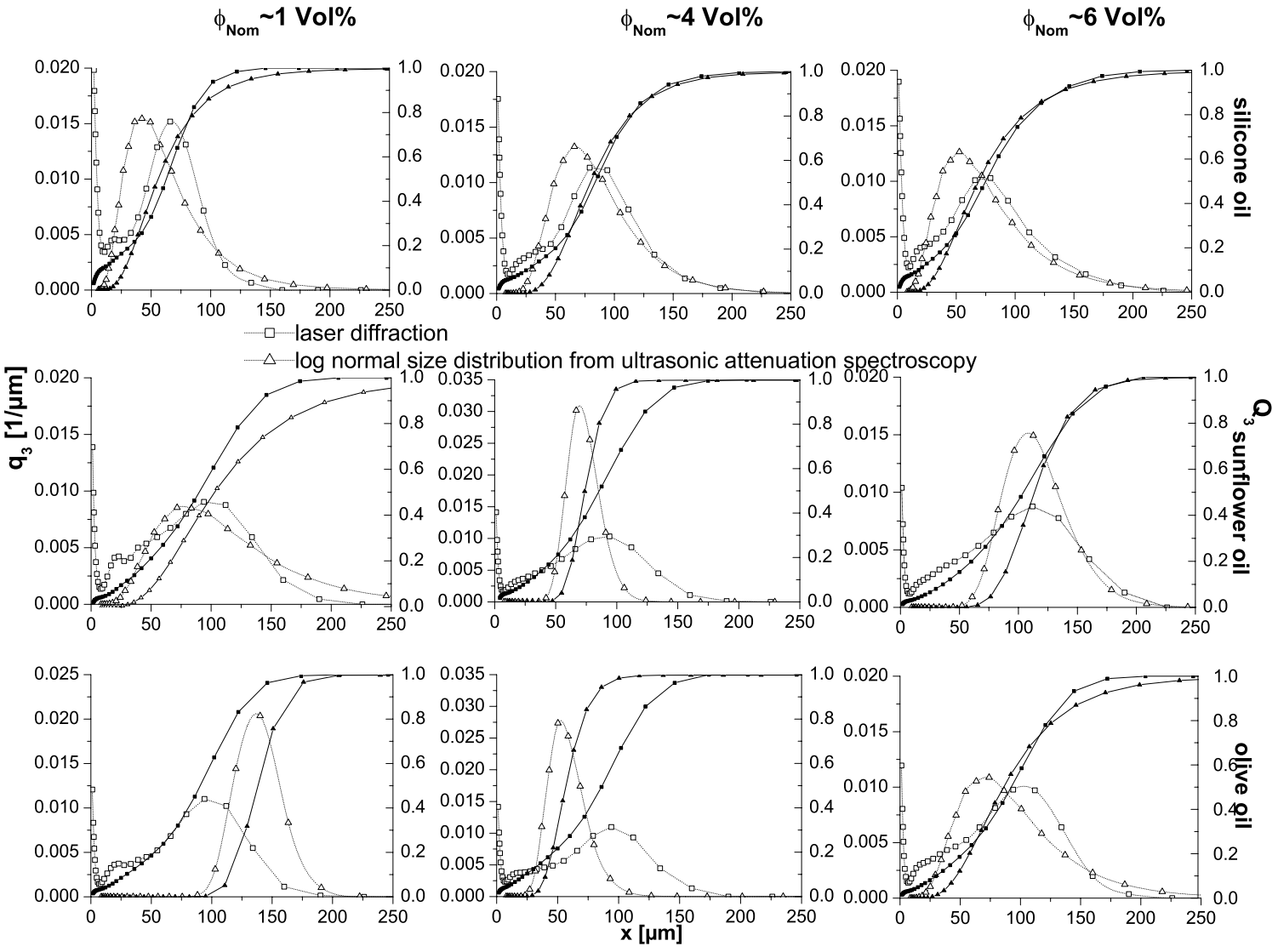
ϕ_{Nom}~1 Vol%
ϕ_{Nom}~4 Vol%
ϕ_{Nom}~6 Vol%
silicone oil
sunflower oil
olive oil
laser diffraction
log normal size distribution from ultrasonic attenuation spectroscopy
q_3 [1/µm]
Q_3
x [µm]

6: Table 1

Table 1: Properties of fluids studied in attenuation experiments

Name	density ρ [kg/m³]	viscosity η [mPas]	bulk modulus K [kg/ms^2]	sound velocity c [m/s]
deionised water	997.2	0.89	$22.109 \cdot 10^8$	1489.00
silicone oil Wacker AK50	957.3	48	$9.434 \cdot 10^8$	992.07
sunflower oil	915.9	50	$19.316 \cdot 10^8$	1452.25
olive oil	909.0	61	$19.180 \cdot 10^8$	1450.88
continuous phase (water+ emulsifier+ stabilizer)	997.3	3.51	$22.386 \cdot 10^8$	1498.23

6: Table 2

Table 2: Volume fractions of dispersed phases

dispersed phase	φ_{Nom} [Vol%]	φ_{bf} [Vol%]	$\lvert \varphi_{Nom} - \varphi_{bf} \rvert$ [Vol%]	deviation [%]
silicone oil	1.02	0.98	0.04	3.92
	4.04	4.09	0.05	1.24
	5.98	5.99	0.01	0.17
sunflower oil	0.98	0.73	0.25	25.51
	4.20	4.52	0.32	7.62
	6.06	6.22	0.16	2.64
olive oil	0.98	0.86	0.12	12.22
	4.04	7.36	3.32	82.18
	5.98	6.60	0.62	10.37